

## Measurement of the $^{235}\text{U}(n,f)$ cross section at n\_TOF from thermal to 170 keV

Simone Amaducci

*Dipartimento di Fisica e Astronomia, Università di Catania, via Santa Sofia 64,  
INFN Laboratori Nazionali del Sud, via Santa Sofia 62, Catania, 95123, Italy  
amaducci@lns.infn.it*

S. Amaducci<sup>1,35</sup>, O. Aberle<sup>6</sup>, J. Andrzejewski<sup>7</sup>, L. Audouin<sup>8</sup>, M. Bacak<sup>9,6,10</sup>, J. Balibrea<sup>11</sup>, M. Barbagallo<sup>2</sup>, F. Bečvář<sup>12</sup>, E. Berthoumieux<sup>10</sup>, J. Billowes<sup>13</sup>, D. Bosnar<sup>14</sup>, A. Brown<sup>15</sup>, M. Caamaño<sup>16</sup>, F. Calviño<sup>17</sup>, M. Calviani<sup>6</sup>, D. Cano-Ott<sup>11</sup>, R. Cardella<sup>6</sup>, A. Casanovas<sup>17</sup>, F. Cerutti<sup>6</sup>, Y. H. Chen<sup>8</sup>, E. Chiaveri<sup>6,13,18</sup>, N. Colonna<sup>2</sup>, G. Cortés<sup>17</sup>, M. A. Cortés-Giraldo<sup>18</sup>, L. Cosentino<sup>1</sup>, L. A. Damone<sup>2,19</sup>, M. Diakaki<sup>10</sup>, C. Domingo-Pardo<sup>20</sup>, R. Dressler<sup>21</sup>, E. Dupont<sup>10</sup>, I. Durán<sup>16</sup>, B. Fernández-Domínguez<sup>16</sup>, A. Ferrari<sup>6</sup>, P. Ferreira<sup>22</sup>, P. Finocchiaro<sup>1</sup>, V. Furman<sup>23</sup>, K. Göbel<sup>24</sup>, A. R. García<sup>11</sup>, A. Gawlik<sup>7</sup>, S. Gilardoni<sup>6</sup>, T. Glodariu<sup>25</sup>, I. F. Gonçalves<sup>22</sup>, E. González-Romero<sup>11</sup>, E. Griesmayer<sup>9</sup>, C. Guerrero<sup>18</sup>, F. Gunsing<sup>10,6</sup>, H. Harada<sup>26</sup>, S. Heinitz<sup>21</sup>, J. Heyse<sup>27</sup>, D. G. Jenkins<sup>15</sup>, E. Jericha<sup>9</sup>, F. Käppeler<sup>28</sup>, Y. Kadi<sup>6</sup>, A. Kalamara<sup>29</sup>, P. Kavragin<sup>9</sup>, A. Kimura<sup>26</sup>, N. Kivel<sup>21</sup>, I. Knapova<sup>12</sup>, M. Kokkoris<sup>29</sup>, M. Krčička<sup>12</sup>, D. Kurtulgiç<sup>24</sup>, S. Lo Meo<sup>3,4</sup>, E. Leal-Cidoncha<sup>16</sup>, C. Lederer<sup>30</sup>, H. Leeb<sup>9</sup>, J. Lerenegui-Marco<sup>18</sup>, S. J. Lonsdale<sup>30</sup>, D. Macina<sup>6</sup>, A. Manna<sup>4,5</sup>, J. Marganiec<sup>7,31</sup>, T. Martínez<sup>11</sup>, A. Masi<sup>6</sup>, C. Massimi<sup>4,5</sup>, P. Mastinu<sup>32</sup>, M. Mastromarco<sup>2</sup>, E. A. Mauger<sup>21</sup>, A. Mazzone<sup>2,33</sup>, E. Mendoza<sup>11</sup>, A. Mengoni<sup>3,4</sup>, P. M. Milazzo<sup>34</sup>, F. Mingrone<sup>6</sup>, A. Musumarra<sup>1,35</sup>, A. Negret<sup>25</sup>, R. Nolte<sup>31</sup>, A. Oprea<sup>25</sup>, N. Patronis<sup>36</sup>, A. Pavlik<sup>37</sup>, J. Perkowski<sup>7</sup>, I. Porras<sup>38</sup>, J. Praena<sup>38</sup>, J. M. Quesada<sup>18</sup>, D. Radeck<sup>31</sup>, T. Rauscher<sup>39,40</sup>, R. Reifarth<sup>24</sup>, C. Rubbia<sup>6</sup>, J. A. Ryan<sup>13</sup>, M. Sabaté-Gilarte<sup>6,18</sup>, A. Saxena<sup>41</sup>, P. Schillebeeckx<sup>27</sup>, D. Schumann<sup>21</sup>, P. Sedyshev<sup>23</sup>, A. G. Smith<sup>13</sup>, N. V. Sosnin<sup>13</sup>, A. Stamatopoulos<sup>29</sup>, G. Tagliente<sup>2</sup>, J. L. Tain<sup>20</sup>, A. Tarifeño-Saldivia<sup>17</sup>, L. Tassan-Got<sup>3</sup>, S. Valenta<sup>12</sup>, G. Vannini<sup>4,5</sup>, V. Variale<sup>2</sup>, P. Vaz<sup>22</sup>, A. Ventura<sup>4</sup>, V. Vlachoudis<sup>6</sup>, R. Vlastou<sup>29</sup>, A. Wallner<sup>42</sup>, S. Warren<sup>13</sup>, C. Weiss<sup>9</sup>, P. J. Woods<sup>30</sup> and T. Wright<sup>13</sup>, P. Žugec<sup>14,6</sup>

<sup>1</sup>INFN Laboratori Nazionali del Sud, Catania, Italy

<sup>2</sup>Istituto Nazionale di Fisica Nucleare, Sezione di Bari, Italy

<sup>3</sup>Agenzia nazionale per le nuove tecnologie (ENEA), Bologna, Italy

<sup>4</sup>Istituto Nazionale di Fisica Nucleare, Sezione di Bologna, Italy

<sup>5</sup>Dipartimento di Fisica e Astronomia, Università di Bologna, Italy

<sup>6</sup>European Organization for Nuclear Research (CERN), Switzerland

<sup>7</sup>University of Lodz, Poland

<sup>8</sup>Institut de Physique Nucléaire, CNRS-IN2P3, Univ. Paris-Sud, Université Paris-Saclay,

F-91406 Orsay Cedex, France

<sup>9</sup>Technische Universität Wien, Austria

<sup>10</sup>CEA Irfu, Université Paris-Saclay, F-91191 Gif-sur-Yvette, France

<sup>11</sup>Centro de Investigaciones Energéticas Medioambientales y Tecnológicas (CIEMAT), Spain

<sup>12</sup>Charles University, Prague, Czech Republic

<sup>13</sup>University of Manchester, United Kingdom

<sup>14</sup>Department of Physics, Faculty of Science, University of Zagreb, Zagreb, Croatia

<sup>15</sup>University of York, United Kingdom

<sup>16</sup>University of Santiago de Compostela, Spain

This is an Open Access article published by World Scientific Publishing Company. It is distributed under the terms of the Creative Commons Attribution 4.0 (CC-BY) License. Further distribution of this work is permitted, provided the original work is properly cited.

- <sup>17</sup>Universitat Politècnica de Catalunya, Spain  
<sup>18</sup>Universidad de Sevilla, Spain  
<sup>19</sup>Dipartimento di Fisica, Università degli Studi di Bari, Italy  
<sup>20</sup>Instituto de Fisica Corpuscular, CSIC - Universidad de Valencia, Spain  
<sup>21</sup>Paul Scherrer Institut (PSI), Villigen, Switzerland  
<sup>22</sup>Instituto Superior Técnico, Lisbon, Portugal  
<sup>23</sup>Joint Institute for Nuclear Research (JINR), Dubna, Russia  
<sup>24</sup>Goethe University Frankfurt, Germany  
<sup>25</sup>Horia Hulubei National Institute of Physics and Nuclear Engineering, Romania  
<sup>26</sup>Japan Atomic Energy Agency (JAEA), Tokai-mura, Japan  
<sup>27</sup>European Commission, Joint Research Centre, Geel, Retieseweg 111, B-2440 Geel, Belgium  
<sup>28</sup>Karlsruhe Institute of Technology, Campus North, IKP, 76021 Karlsruhe, Germany  
<sup>29</sup>National Technical University of Athens, Greece  
<sup>30</sup>School of Physics and Astronomy, University of Edinburgh, United Kingdom  
<sup>31</sup>Physikalisch-Technische Bundesanstalt (PTB), Bundesallee 100, 38116 Braunschweig, Germany  
<sup>32</sup>Istituto Nazionale di Fisica Nucleare, Sezione di Legnaro, Italy  
<sup>33</sup>Consiglio Nazionale delle Ricerche, Bari, Italy  
<sup>34</sup>Istituto Nazionale di Fisica Nucleare, Sezione di Trieste, Italy  
<sup>35</sup>Dipartimento di Fisica e Astronomia, Università di Catania, Italy  
<sup>36</sup>University of Ioannina, Greece  
<sup>37</sup>University of Vienna, Faculty of Physics, Vienna, Austria  
<sup>38</sup>University of Granada, Spain  
<sup>39</sup>Department of Physics, University of Basel, Switzerland  
<sup>40</sup>Centre for Astrophysics Research, University of Hertfordshire, United Kingdom  
<sup>41</sup>Bhabha Atomic Research Centre (BARC), India  
<sup>42</sup>Australian National University, Canberra, Australia

Published 23 September 2020

The  $^{235}\text{U}(n,f)$  cross section plays a key role for nuclear physics due to its widespread use as a standard reference for neutron cross section measurements and for neutron flux measurements. Recent experimental data of the fission cross section have suggested the presence of discrepancies around 6–8% with respect to the most used libraries, precisely in the range between 10 keV and 30 keV. In order to shed light on this disagreement, an accurate measurement of the  $^{235}\text{U}(n,f)$  fission cross section has been performed at n\_TOF facility @CERN, using the standard reactions  $^6\text{Li}(n,t)$  and  $^{10}\text{B}(n,\alpha)$  as reference. A custom experimental setup based on a stack of silicon detectors sandwiched between pairs of  $^{235}\text{U}$ ,  $^6\text{Li}$  and  $^{10}\text{B}$  targets, has been installed along the neutron beam line to intercept the same neutron flux, allowing the detection of the fission fragments and the products of the reference reactions at the same time. Such a technique allows calculation of the cross section via the “ratio method”, by normalizing the  $^{235}\text{U}(n,f)$  reaction yields with respect to the reference reactions and to the recommended data in the IAEA libraries; in particular, the integral between 7.8 and 11 eV has been chosen. Accurate Monte Carlo simulations have allowed evaluation of the neutron absorption in the different layers, as well as the detection efficiency of each detector. The data are in excellent agreement with the standard values and highlight the overestimation of the  $^{235}\text{U}(n,f)$  cross section between 9 and 18 keV in the most recent libraries.

*Keywords:* Standard; cross-section; neutrons; uranium; fission; n\_TOF.

## 1. Introduction

Recently, a large number of applications have demanded new and more accurate data for neutron induced reactions. The International Atomic Energy Agency (IAEA) defines as standard a small group of neutron cross sections (see Refs. 1 and 2), known with high

accuracy in a well-defined neutron energy interval, that are used as a reference for several neutron cross section measurements, whose precision therefore depends on the accuracy of the standards. Among them, the  $^{235}\text{U}$  fission cross section is one of the most used, mainly because of the large energy interval in which it is a standard: at thermal energy and in the interval between 150 keV and 200 MeV. Even if it is not a standard between thermal and 150 keV, this cross section is currently used as a reference. Thanks to this wide energy range, the  $^{235}\text{U}(n,f)$  reaction is therefore the most used reference for fission and capture cross section measurements, in particular of actinides. This feature makes this cross section directly interesting for the design of new-generation fission reactors in the keV region, in particular for the Accelerated-Driven Subcritical reactors, and in the field of nuclear waste burning. The uncertainty of the  $^{235}\text{U}(n,f)$  cross section is typically lower than 5%, but a discrepancy in the 10 to 30 keV range has been observed between new experimental data and the evaluated libraries,<sup>3</sup> due to possible overestimation of the latter.

The consequent requirements of new data to verify these disagreements has triggered an experiment, performed in 2016, to measure the  $^{235}\text{U}(n,f)$  fission cross section from thermal to 170 keV with high accuracy. The measurement was performed at the n\_TOF facility operating at CERN by using the standard reactions  $^6\text{Li}(n,t)$  and  $^{10}\text{B}(n,\alpha)$  as reference reactions. The high energy resolution (up to  $10^{-4}$ ) neutron beam and the high instantaneous flux available in this facility is well suited to measure the cross section in the energy range of interest, with an accuracy well below 5%. A custom experimental apparatus based on in-beam silicon detectors has been carried out, allowing for the first time the use of silicon detectors at n\_TOF for fission cross section measurements.

The results have confirmed the overestimation of the cross section by the most recent evaluated libraries between 9 and 18 keV. Furthermore, the measurement hinted at the presence of structures in the energy interval between 2.2 and 4 keV that currently are not included in the libraries. This new data improves the accuracy of the  $^{235}\text{U}(n,f)$  cross section, thus increasing its role as a reliable reference for neutron induced nuclear reactions. More details about the analysis are provided in the full article in Ref. 4.

## 2. Experimental Setup

The measurement was performed in the first experimental area (EAR1) of the n\_TOF facility at CERN.<sup>5</sup> Here a pulsed neutron beam with a high instantaneous flux ( $10^5$ – $10^6$  n/bunch) is produced by the spallation process, induced by the 20 GeV protons accelerated by the Proton Synchrotron interacting inside a lead target. The energy range of the neutrons arriving in the experimental area after a flight path of 183.49(2) m is from thermal to 1 GeV, with an excellent energy resolution of  $10^{-4}$ . The energy of neutrons is measured by time of flight techniques.

Three pairs of reaction targets have been used in order to measure the  $^{235}\text{U}(n,f)$  reaction at the same time as the IAEA standards,  $^6\text{Li}(n,t)$  and  $^{10}\text{B}(n,\alpha)$ . Six  $5\times 5$  cm<sup>2</sup>

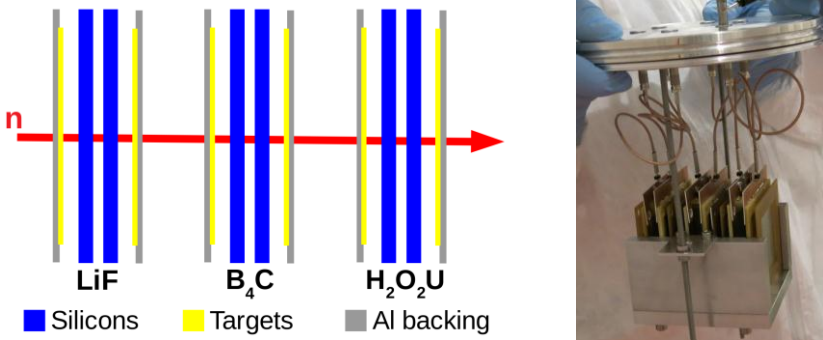


Fig. 1. Drawing and photo of the setup used for the measurement.

Table 1. Characteristics of the six samples; all the active targets are deposited on an aluminum backing.

Deposit	Size (mm)	Thickness ( $\mu\text{m}$ )	Backing	Enrichment
LiF	Square 47x47 mm	1.97 (3)	Al 50 $\mu\text{m}$	95%
B <sub>4</sub> C	Square 70x70 mm	0.080 (5)	Al 18 $\mu\text{m}$	99%
H <sub>2</sub> O <sub>2</sub> U	Circular with 40 mm diameter	0.1450 (16)	Al 250 $\mu\text{m}$	99.999%

silicon detectors with 200  $\mu\text{m}$  thickness have been arranged, each one close to the corresponding target as shown in Fig. 1, in order to detect the reaction products emitted in the forward and backward direction with respect to the neutron beam. This configuration guarantees a sufficient level of redundancy and compensates (to a large extent) the forward/backward emission asymmetry due to the large geometric efficiency. Silicon detectors have been chosen because of their high energy resolution, which is required to discriminate the reaction products and efficiently reject the background. Moreover the compactness of the setup implies that all the samples share the same neutron beam, apart from small differences due to the absorption in the dead layers. This means that the ratio between the reaction yields is proportional to the ratio between the cross sections, and the so called “ratio method” can be used to measure the fission cross section.

As was mentioned before, two samples with two corresponding detectors were used for each reaction, named according to the sample “Li”, “B” and “U”. Additionally we are referring to the detector in the forward direction with the suffix “\_f” and to the one in the backward direction with “\_b”. The properties of samples are reported in Table 1. It is important to note that the thicknesses of all the samples are small enough to prevent the self-absorption effects and use the “thin sample” approximation.

### 3. Data Analysis

The accuracy of measurement of the neutron kinetic energy depends on the precise calibration of the flight path used to convert the time of flight spectra into neutron

energy. In our case, the calibration was performed via a linear fit of the time-to-energy relation for forty prominent resonances between 2 and 35 keV. The calibration was then refined by minimizing the  $\chi^2$  between experimental data and ENDF-B/VIII evaluation in a small interval around the best value of the fit.

The stability of the detectors during the whole measurement has been checked, with particular care to those coupled with the  $^{235}\text{U}$  samples that were exposed to fission fragments and alpha particles produced by  $^{235}\text{U}$  decay. The data have evidenced no significant deviation of the silicon detectors performances that worked very well during the complete measurement.

The “ratio method” has been used in order to be independent of any flux evaluations done with other devices, thus making the measurement absolutely self-consistent. In particular the  $^{235}\text{U}(n,f)$  cross section was obtained with respect to the reaction references  $^6\text{Li}(n,t)$  and  $^{10}\text{B}(n,\alpha)$ , by the following equation:

$$\sigma_{235U} = \frac{C_{235U} f_{ref} \rho_{ref} \epsilon_{ref}}{C_{ref} f_{235U} \rho_{235U} \epsilon_{235U}} \sigma_{ref} , \quad (1)$$

with  $C_X$  the number of counts for a given sample  $X$ ,  $\rho_X$  the areal density of the sample,  $f_X$  the neutron beam fraction hitting the sample and  $\epsilon_X$  the detection efficiency of the corresponding reaction products.

The experimental count rates  $C_X$  were obtained by selecting the events with high accuracy, using the tritons for the  $^6\text{Li}(n,t)$  reaction, the alpha particles for  $^{10}\text{B}(n,\alpha)$  and the fission fragments for  $^{235}\text{U}(n,f)$ . For each detector, an energy threshold was chosen by the two-dimensional scatter plots, with the deposited energy as a function of the neutron energy. The experimental thresholds for the  $^6\text{Li}$  and  $^{10}\text{B}$  reactions took into account the kinetic energy of the incident neutron and the angular distribution of reaction products. As can be seen in Fig. 2, starting from a neutron energy of a few keV, the threshold of the detectors in the forward direction increases, while it decreases for the detectors in the backward direction. Thanks to the large fission Q-value (around 200 MeV), the threshold to discriminate the fission fragments from the natural alpha decay of  $^{235}\text{U}$  has been maintained constant. As examples, the plots for backward  $^6\text{Li}(n,t)$  and  $^{235}\text{U}(n,f)$  are shown in Fig. 2.

### 3.1. Monte Carlo simulations

The correction factors needed to compensate the small differences in the neutron flux impinging on each target have been evaluated by means of a GEANT4 Monte Carlo code, where the full experimental apparatus has been implemented. A realistic n\_TOF neutron flux, with a Gaussian transverse profile of  $\sigma = 7$  mm, has been used to calculate the correction factors via the ratio of the energy spectra of the neutrons hitting each target to the generated ones. The results are shown in Fig. 3, where the fractions of the neutrons to the total ones are plotted for the three targets in the backward direction as a function of

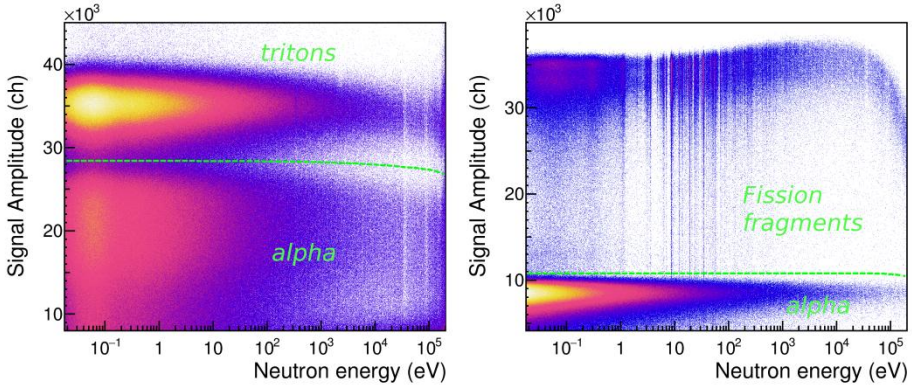


Fig. 2. Two-dimensional scatter plots of backward detector coupled with a  ${}^6\text{Li}$  sample (left) and a forward detector coupled with a  ${}^{235}\text{U}$  sample (right).

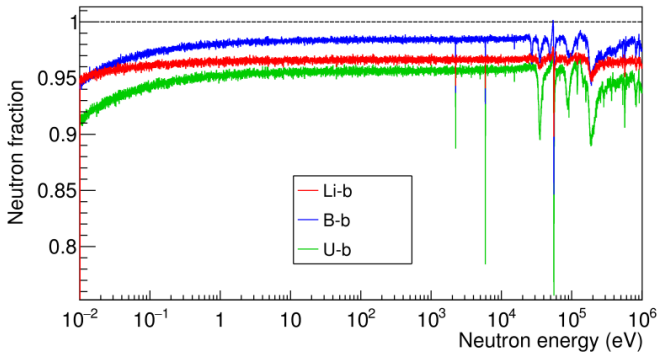


Fig. 3. Correction for the absorption of neutrons in the materials placed along the beam for the backward detectors.

their energy. The correction is in general quite small, except at the thermal region where the  ${}^6\text{Li}(n,t)$  and  ${}^{10}\text{B}(n,\alpha)$  cross sections are larger, and at the aluminum capture resonance at 5.9 keV.

A further GEANT4 simulation was done to estimate the efficiency for  ${}^6\text{Li}(n,t)$  and  ${}^{10}\text{B}(n,\alpha)$  reactions. For the  ${}^{235}\text{U}(n,f)$ , reaction, the simulation was not necessary, because its efficiency is constant over the whole neutron energy range. For  ${}^6\text{Li}$  and  ${}^{10}\text{B}$ , the efficiency is mainly determined by the angular distribution of the reaction products provided by ENDF-B/VIII<sup>6</sup> that has been used in the simulation. The calibrated experimental data and the experimental threshold used to select the reaction products were included in the simulation.

The efficiency estimated with the simulation for the reactions  ${}^6\text{Li}(n,t)$  and  ${}^{10}\text{B}(n,\alpha)$  are shown in Fig. 4. As expected, the efficiency increases with the neutron energy for the

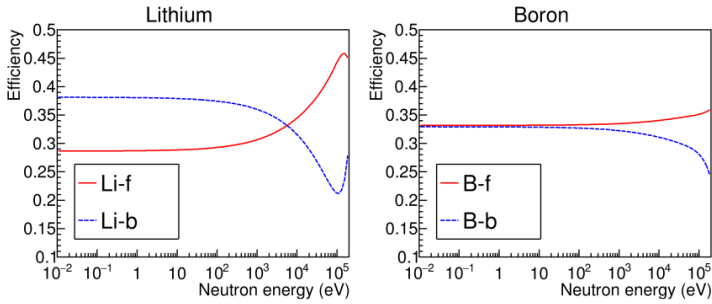


Fig. 4. Estimated efficiency for  $^6\text{Li}(n,t)$  (left) and  $^{10}\text{B}(n,\alpha)$  (right), for the forward (blue) and backward (red) detectors.

forward detectors, while it decreases for the backward ones. The dependence on the neutron energy is greater for the  $^6\text{Li}$  reaction due to the strong anisotropic emission of products in the keV region for the  $^6\text{Li}(n,t)$  reaction. In particular, from a few keV, the tritons are mainly emitted in the forward direction, reaching an efficiency up to 45%. For the  $^{10}\text{B}(n,\alpha)$  reaction, the forward/backward differences are smaller since there are not such large anisotropic emissions, and the differences mainly depend on the incident neutron kinetic energy.

### 3.2. Reference consistency and normalization

The reliability of the measurement is assured by the two independent standard cross sections  $^6\text{Li}(n,t)$  and  $^{10}\text{B}(n,\alpha)$  used as reference. This has allowed a check of the consistency of the references with respect to each other in order to verify the validity of the efficiency and the absorption corrections with a high accuracy. The correction for absorption and efficiency described in the previous section has been applied to the experimental count-rates; then for each reaction, the data from the forward and backward detectors have been combined using a weighted average.

The consistency between the standard references has been evaluated by comparing the ratio between the count rates of lithium and boron, after the corrections for efficiency and absorption, with the ratios of the cross sections provided by ENDF-B/VIII. The experimental and expected ratios are shown in Fig. 5, where the experimental data are in good agreement with the foreseen values. Once the consistency of the two standard references was verified, the data collected with lithium and boron were divided by the corresponding cross section and combined using again a weighted average.

Knowing the efficiencies of the reference reactions, the  $^{235}\text{U}(n,f)$  cross section can be calculated with the “ratio method” by means of the Eq. (1), even if a suitable normalization is required to take into account the areal densities and the  $^{235}\text{U}(n,f)$  efficiency. To do this, the range between 7.8 and 11 eV has been chosen as recommended

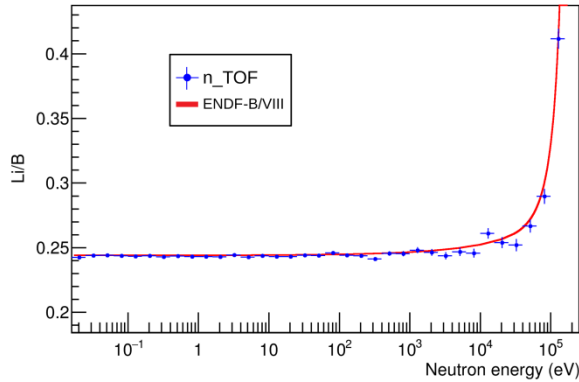


Fig. 5. Ratio between experimental count ratio of lithium and boron (blue) compared with expected values provided from standard libraries (red).

in Ref. 1, in which the correction due to the absorption of neutrons is minimal. Furthermore we have verified the agreement with the values at thermal energy, where all three cross sections are standards. The ratio between thermal and the [7.8,11] eV integral has been compared with the IAEA evaluations data and the major libraries, showing a good agreement.

### 3.3. Comparison with libraries

The  $^{235}\text{U}(n,f)$  cross section has been obtained using the two standard reactions,  $^6\text{Li}(n,t)$  and  $^{10}\text{B}(n,\alpha)$ , and normalizing the shape of the cross section to the integral between 7.8 and 11 eV. The resulting n\_TOF cross section has been compared with the most recent evaluated libraries, namely ENDF-B/VIII<sup>6</sup> and JEFF3.3,<sup>7</sup> and with the last indication provided by IAEA in Ref. 1. This comparison has been made over significant integral intervals in the keV region where previous discrepancies were found.

The ratio of n\_TOF data and the libraries is reported in Fig. 6, together with the deviation in standard deviation units. Over the interval from 9 to 18 keV, in a region where discrepancies have already been observed, the deviation of the n\_TOF data from all the references considered is more than three standard deviations; in terms of percentage, this deviation is around 4–5%. It is important to note that this deviation is not present in the 18 to 30 keV integral, and if we consider the full interval from 9 to 30 keV, the deviation is no longer statistically significant. The reliability of the n\_TOF data is further guaranteed by the good agreement in the 150 to 170 keV interval, since in this energy range the  $^{235}\text{U}(n,f)$  cross section is again considered a standard.



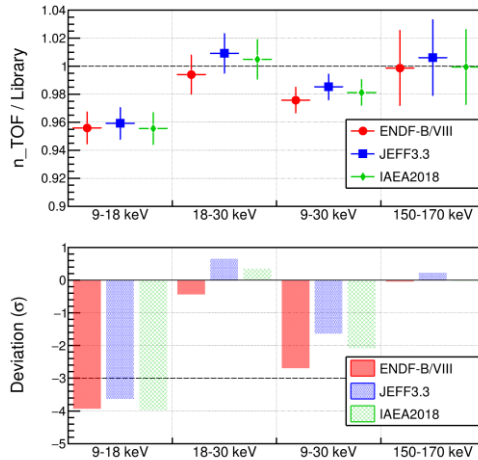


Fig. 6. Top panel: ratio between  $n_{\text{TOF}}$  measured fission cross section in four integrals and the values provided by major libraries. Bottom panel: deviation of  $n_{\text{TOF}}$  integral from the libraries expressed in units of standard deviation.

#### 4. Conclusions

A very accurate measurement of the  $^{235}\text{U}(n,f)$  cross section was performed at  $n_{\text{TOF}}$  from thermal to 170 keV, using the standard reactions  $^6\text{Li}(n,t)$  and  $^{10}\text{B}(n,\alpha)$  as reference. For the measurement, a dedicated setup based on in-beam silicon detectors was used. The experimental data have been corrected for neutron absorption and detection efficiency, and the consistency of the two standard references has been verified during the analysis.

The results indicate the presence of an overestimation in all the major standard libraries in the energy interval from 9 to 18 keV. The reliability of the measured cross section is assured by the agreement with the libraries in the energy range where  $^{235}\text{U}(n,f)$  is considered a standard, namely at thermal energy and from 150 keV to 170 keV.

The performance of silicon detectors exposed to the  $n_{\text{TOF}}$  neutron flux and to fission fragments remained stable throughout the campaign; thus, an apparatus based on silicon detectors can be used for a systematic study of actinide fission cross sections at  $n_{\text{TOF}}$ , which are currently of great interest for the design of new-generation reactors and nuclear waste burning.

#### References

1. A. D. Carlson *et al.*, *Nucl. Data Sheets* **148**, 143 (2018).
2. A. D. Carlson *et al.*, *Nucl. Data Sheets* **110**, 3215 (2009).
3. M. Barbagallo *et al.*, *Eur. Phys. J. A* **49**, 156 (2013).
4. S. Amaducci *et al.*, *Eur. Phys. J. A* **55**, 120 (2019).
5. C. Guerrero *et al.*, *Eur. Phys. J. A* **49**, 27 (2013).
6. D. A. Brown *et al.*, *Nucl. Data Sheets* **148**, 1 (2018).
7. <https://www.oecd-nea.org/dbdata/jeff/jeff33/>.